

Towards Modelling Elastic and Viscoelastic Seismic Wave Propagation in Boreholes

NA WANG, DONG SHI, BERND MILKEREIT

Department of Physics, University of Toronto, Toronto, Canada M5S 1A7

Summary

We are studying elastic seismic wave propagation in shallow marine and fluid-filled borehole settings. Body waves and Stoneley waves are controlled by strong contrasts in physical properties - in particular, the S wave velocities in elastic formation. In addition, location of sensors within the fluid layer, at the interface or within the elastic formation controls measured amplitude and phase of the seismic wave field. To study these effects, we propagate the wave field using Finite Differential (FD) method. Using divergent and curl operations on the displacement wave field, we can separate and identify Stoneley wave, P and S wave arrivals.

Introduction

Until recently, the cased multilayered and purely fluid-filled boreholes have been studied for propagation and dispersion characteristics of guided waves by using specialized Bessel functions in cylindrical coordinates (Cheng, 1981; Kenneth, 1984). The relationship of formation parameters: velocity, density ratio, and Poisson's ratio in cylindrical bores, have been derived from the elastic wave equation by Biot (1952). By applying this to full sonic log data, numerical errors have been found in density inversion (Milkereit B., 2005). Viewing 3D boreholes from another aspect, full waveform sonic logs can be viewed as being analogous to shallow-water marine sediment (Kugler et al., 2005), as long as scale is considered. In this study, we model elastic wave propagation in shallow-water marine sediment and 2D fluid-filled boreholes. As a second step, we will consider the attenuation and heterogeneity in a 3D borehole FD method and invert the seismogram based on analysis of aforementioned two models.

There are two kinds of body waves propagating in elastic media, P and S wave, which may be converted to other while crossing interfaces. Waves propagating along the water-formation boundary include: Stoneley waves, P and S surface waves. Stoneley waves move slower, therefore arrive just after shear waves. They also exhibit high amplitude, depending on the permeability of the formation, but decrease rapidly as the depth from the interface increases at a length comparable to its wavelength. Pseudo-Rayleigh waves are observed when the formation is hard rock which has a shear wave velocity larger than the P wave in the overlying water. Pseudo-Rayleigh waves are also called shear surface waves or normal modes which follow a shear body wave in a seismogram.

	Vp m/s	Vs m/s	density kg/m ³	fluid density/rock density	Vp/Vs	Poisson's ratio
water	1500	0	1000	1	—	0.5
soft sediment	2000	700	2000	0.5	2.86	0.43
hard sediment	4000	2000	2200	0.45	2	0.33

Table 1, Physical parameters of fluid-solid models.

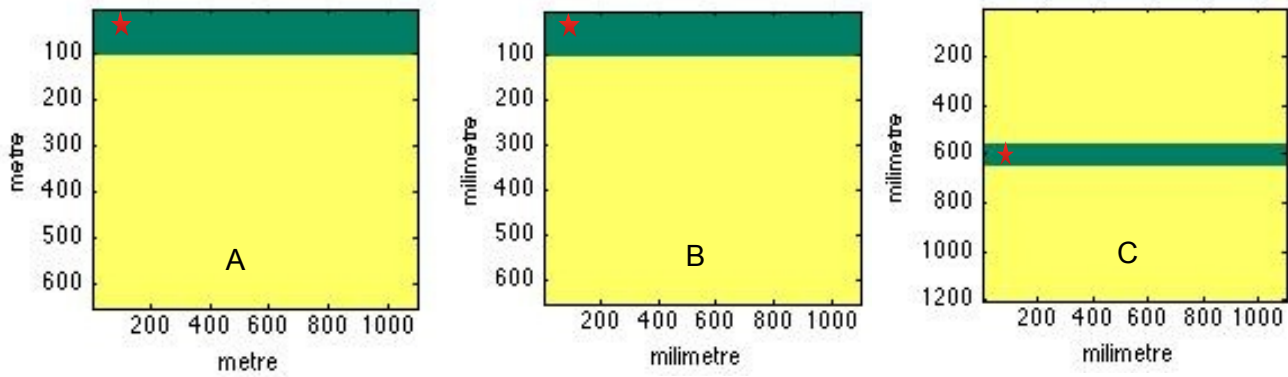


Fig 1: Model A is shallow-water marine sediment in metre scale; Green media means water layer, yellow is formation, and red star is seismic source. Model B is the same as A except axes are set to be millimetre scale (the borehole simulation); Model C represents the fluid-filled borehole in the 2D plane. Receivers coupled to elastic media are put both within the water layer, formation and at the interface.

Methodology

We assume shallow marine sediments and borehole formations are homogeneous, isotropic and nonporous. We simplify the 3D borehole by taking a vertical plane through the axis of a horizontal borehole, as shown in Fig 1 model C. The parameters are shown in Table 1. We use 2D finite difference (Bohlen, 2002) for the theoretical numerical calculations. For higher accuracy, an 8th order time-space finite differential is applied in standard staggered grid. The seismic wavelet is a Ricker wavelet, with 0.1 seconds duration. Three component geophones oriented in x,y,z directions measure the pressure which is achieved by particles' spacial displacement. The transfer of displacement to pressure can be written as:

$$\epsilon_{ij} = \frac{1}{2}(u_{i,j} + u_{j,i}), \sigma_{ij} = \lambda \theta \delta_{ij} + 2\mu \epsilon_{ij}$$

with ϵ_{ij} is strain, σ_{ij} is stress, $\theta = \epsilon_{ii}$

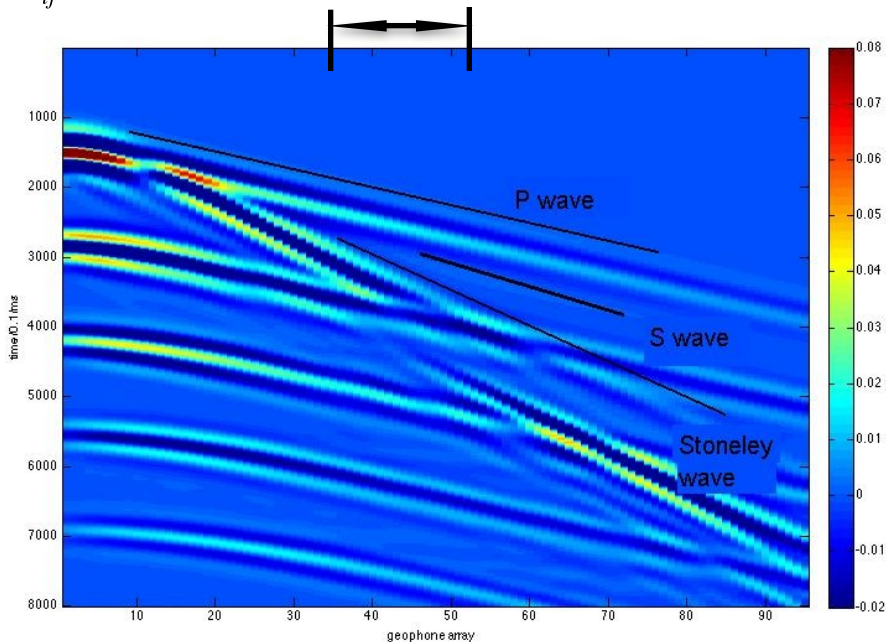


Fig 2, Total seismogram of model A with “hard” sediment, the geophone array is located 10 m below water bottom. Every event is coupled with a ghost, and black lines highlight arrival times of every event. Limited offset range of seismic data recorded by a typical full waveform sonic log is indicated by the arrow.

As the diameter of a borehole is on the order of the seismic wavelength and the reflection coefficients at the wall are -1, there occurs a resonance phenomenon. This is the same in marine case when we change the scale of water layer depth. Critical parameters for seismic wave propagation are: the ratio of P wave velocity in the fluid and S wave velocity in the solid, the density contrast between fluid and solid, and the seismic wavelength to borehole diameter ratio. In model A, the source central frequency is changed from 10 to 30 Hz, which leads to variation of the wavelength and resultantly Stoneley wave velocity. The data show that as the wavelength increases compared to the depth of the water layer, or borehole's diameter, there is a decrease especially when density ratio is high. Furthermore, the location of the source affects the seismograms significantly. Even the location of sensors, for example in water, right at the interface or within the elastic formation, results in different kinds of waveforms in the displacement data. The type of sensors is also important, for example, hydrophones only detect pressure. But in numerical modelling, we simulate working theory of the geophones, and calculate both vector and horizontal components of displacement.

This concentrates on the strong parameter contrasts between the fluid and elastic formations. Fig 2 is the pressure component of the geophones in hard formation setting and receivers are located in formation 10 m below interface, we got pretty weak S wave and Stoneley wave's velocity is around 1780 m/s in hard formations and 611 m/s in soft. FD snapshots Fig 3 show gradient and curl components at around 400 ms. Since S wave velocity in formation is larger than P wave velocity in water, Pseudo-Rayleigh and head P waves are received when geophones are placed on the boundary, as indicated in Fig 3(a). The wavelengths of P head wave and P body wave indicates strong velocity ratio of water and sediment. At nearly the same time, Stoneley wave departs from the S wave, exhibiting high amplitude which is very clearly in Fig 3(b). Fig 4 are the data from a single geophone in both "hard" and "soft" formation cases. Since P and S components are the gradient and curl of particle displacement respectively, while the total data is the pressure on the geophones, the amplitudes varies significantly. The black boxes in the upper right corner are zoomed in, indicating P and S waves are the first arrivals. The Stoneley arrives at around 200 ms with high amplitude compared to weak S wave. Following events are multiples reflected from the free water surface.

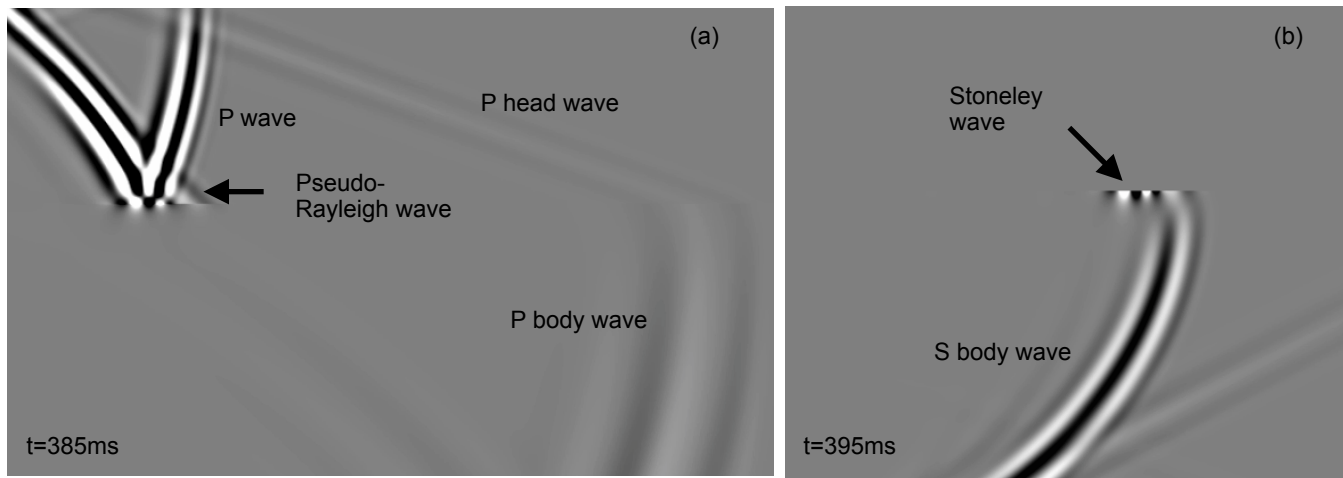


Fig 3, Two snapshots of a wave propagating in a "hard" elastic formation. (a) shows divergent of displacement data and (b) shows curl of displacement data.

Although we are using model A, which has broadband data, results are the same for model B, as long as the central frequency is set to be 1:1000. Since the geophone array in a marine setting is usually hundreds of metres long, marine seismic data provides broadband information on large horizontal sediment environments. However, the number of geophones in a full waveform sonic log is quite limited,

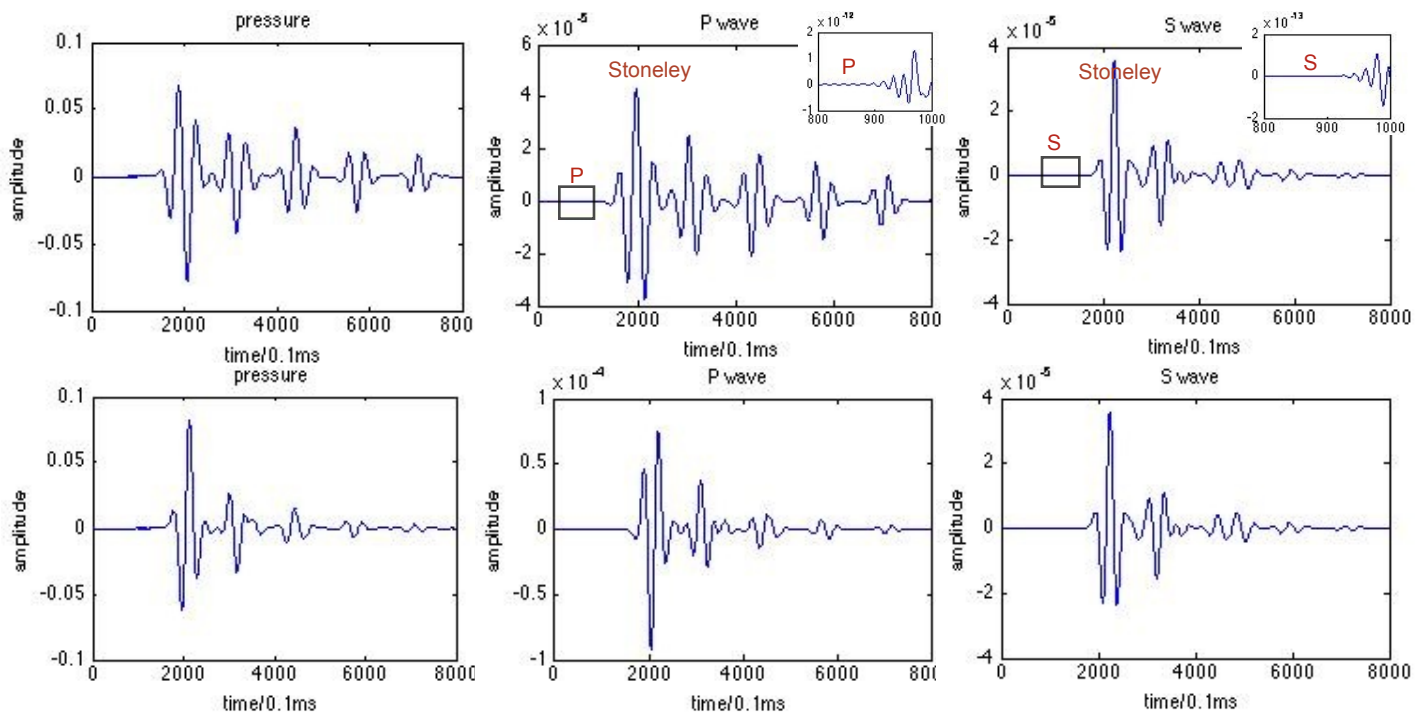


Fig 4, The first row is hard sediment setting, the second is soft. They all come from the same geophone which is 10 m below water bottom, 180 m horizontally away from the source. The central frequency is 20 Hz, and small figures in upper right corner are zoomed in pictures of first arrivals in divergent and curl of displacement data which have much smaller amplitudes than Stoneley wave. P and S waves' arrival time are near 0.09 ms.

the seismogram can be treated as part of the full marine sediment waveform, as the offset range indicated by arrow in Fig 2. These conclusions can be applied to both sides of the borehole wall in model C.

Conclusions

Here we study wave propagation in shallow-water marine sediments and 2D boreholes with elastic formation. The hard and soft formations control Stoneley wave's phase velocity and waveform. Different waveforms and change of wavelength from water to formation are clearly seen in snapshots. The frequency variation contributes to the wavelength and phase velocity of Stoneley waves with certain characteristic parameters. In our future work, formation's attenuation and heterogeneity will be discussed in the 3D borehole problem and inversion will be considered based on these results.

Acknowledgements

This work was finically supported by Natural Sciences and Engineering Research Council of Canada (NSERC). The Sofi 2D FD software used in this study was developed by Thomas Bohlen.

References

Biot MA. Propagation of elastic waves in a cylindrical bore containing a fluid. *Journal of Applied Physics*, 1952, 23(9): 997-1005.

Bohlen T. Parallel 3-D viscoelastic finite difference seismic modelling[J]. *Computers & Geosciences*, 2002, 28(8): 887-899.

Cheng C H, Toksöz M N. Elastic wave propagation in a fluid-filled borehole and synthetic acoustic logs. *Geophysics*, 1981, 46(7): 1042-1053.

Crain E R, Eng P. How many acoustic waves can dance on the head of a sonic log. Canadian well logging society publication, [www. spec2000. net/freepubs/AcousticWaves. pdf](http://www.spec2000.net/freepubs/AcousticWaves.pdf), 2004.

Kugler S, Bohlen T, Bussat S, et al. Variability of Scholte-wave dispersion in shallow-water marine sediments. *Journal of Environmental & Engineering Geophysics*, 2005, 10(2): 203-218.

Milkereit B, Ji J. Extraction of Stoneley Waves from Full Waveform Sonic Data//67th EAGE Conference & Exhibition. 2005.

Tubman K M, Cheng C H, Toksoez M N. Synthetic full waveform acoustic logs in cased boreholes. *Geophysics*, 1984, 49(7): 1051-1059.